BNAM2012
Joint Baltic-Nordic Acoustics Meeting
June 18th - 20th 2012 Odense, Denmark

Edge diffraction implementation by semi-transparent surfaces in geometrical acoustics

Anders Isebakke
Brekke & Strand akustikk AS, P.O. Box 1024 Hoff, 0218, Norway, anders.isebakke@brekkestrand.no

In various commercial acoustic software, geometrical acoustics (GA) is the basis for prediction of the sound field calculations. However, a great disadvantage of this method is that GA is unable to handle diffraction effects. Further, some extended methods, still based on GA assumptions, have been developed to successfully include diffraction. However, the subsequent calculations have been found hard to implement in existing acoustic software. This paper presents an alternative method for diffraction modelling, based on an idea that takes advantage of a defined semi-transparent coefficient assigned to the surface of the obstructing object of a given edge diffraction case.

1 Introduction

When dealing with complex geometric situations *geometrical acoustics (GA)* is an efficient method for solving the wave equation. However, the disadvantage of this method is that it has certain limitations – among them not being able to handle diffraction phenomena in a proper way. Because sound waves are regarded as rays the phase quality of the wave nature is ignored, which often results in low frequency errors as interference patterns often occur and affect this frequency region. Previous studies [1] have been published regarding how edge diffraction successfully can be implemented in GA calculations. However, an often introduced complexity in the consecutive calculation algorithms has made it somewhat inconvenient to implement these previously proposed modelling techniques into commercially available GA software.

More recently, in *Dammerud's* [2] PhD thesis a smart and easily implemented trick was employed in the GA software CATT-Acoustic in order to mimic diffraction phenomena of sound propagation through a symphony orchestra. Briefly, diffraction was implemented by claiming that the sound energy propagates *through* the obstructing objects rather than around them. In principle, this means that diffraction is handled as a property of the obstructing object rather than a property of the wave nature. Even though such a mimetic diffraction implementation will introduce some errors compared to the physical nature of wave propagation, the method is still of further interest – both since it is very efficient, and because highly accurate results often is outside the scope of interest in practical engineering acoustics. Further, a research by *Isebakke* [3] supported the same applied mimetic modelling technique in a study that aimed to simulate the locally perceived acoustic conditions in a public hall audience seating area. Also Isebakke's research revealed somewhat convincing results, and consequently a general potential in the semi-transparent diffraction modelling technique was ensured.

However, the drawback in both *Dammerud* [2] and *Isebakke* [3] is that their results were achieved in a somewhat tentatively proceeding form of research, where available parameters in the simulations were utilized in order to optimally calibrate the model relative to a reference result. Accordingly, at this point it would be of interest to obtain a more in-depth mathematical linkage between the true physical diffraction behavior and the semi-transparent modelling technique.

2 Theory

2.1 Geometrical acoustics (GA)

In short, ray-tracing [4] regards sound propagation as rays travelling normal to the wave front. This is implemented by a defined point source that sends out a large number of rays distributed in all directions. Each ray then represents a certain angle of a spherical wave. Subsequently, all rays are traced through their travel until all energy has died out. Energy is lost due to spherical propagation damping, or when rays hit obstructing objects that are dedicated an absorption coefficient α set between *0* (no absorption) and *1* (total absorption). Non-rigid surfaces are implemented by a dedicated scattering coefficient s set between *0* and *1* with a corresponding number of rays specularly and randomly reflected. Finally, a receiver of a given spherical expansion is employed, being hit by a stochastic number of rays.

Indeed, one simplified way to describe how the ray-tracing method builds an impulse response is by employing the signal processing multipath transmission equation:

$$h(n) = \sum_{k=1}^{K} c_k \delta(n - n_k) \tag{1}$$

where K is the number of rays sent out by the source, c_k is the energy contribution of ray k as it strikes the receiver, and n_k is the the sample number for when ray k strikes the receiver.

2.2 Infinite noise barrier edge diffraction

In this paper a hard rigid infinite noise barrier on a totally absorptive floor (otherwise free-field conditions) is studied. A simple geometrical cross-section of this given case can be seen in Figure 1. The presented variables and their notations will be frequently referred to trough this paper.

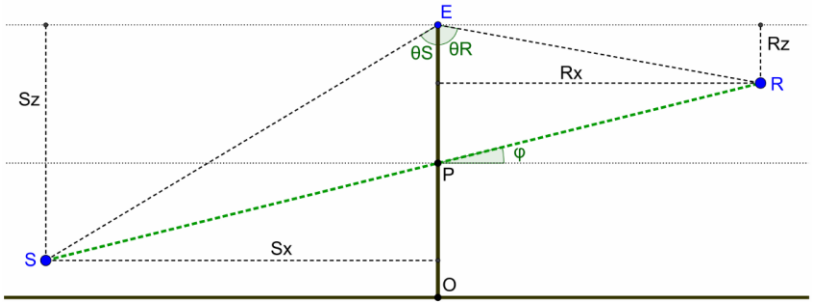

Figure 1: The infinite noise barrier geometry

A typical impulse- and frequency response of such a noise barrier case can be seen in Figure 2. As can be seen, the impulse response appears as a slightly time-smeared impulse. The frequency response slope tends to decrease for an increased frequency, similar to a low pass filter, which indeed agrees with our daily experience.

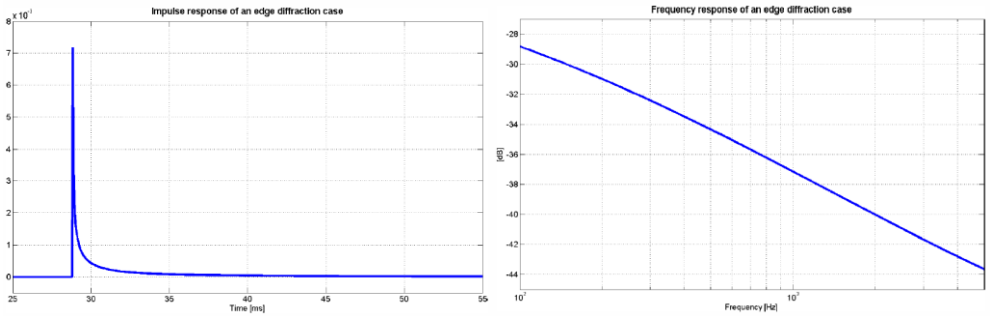

Figure 2: Typical impulse- and frequency response of a noise barrier case. The receiver is located in the shadow zone

3 Method

3.1 Semi-transparent division and the *n*th sample barrier intersection area

Dammerud [2] took advantage of a *semi-transparent* quality that can be dedicated to surfaces in GA. This quality can be implemented by a transparency coefficient τ defined specifically for each octave band. It's range goes from $\tau = 0$ (zero transmission, only reflected and absorbed energy) to $\tau = 1$ (full transparency, no reflected energy) [5, 6].

Now, in order to mime noise barrier edge diffraction it turns out essential to develop a somewhat functional design algorithm of this semi-transparent quality. One possible action will then be to divide the total area of the noise barrier surface S_{tot} into a number of equally large subareas and then dedicate each subarea a suitable transmission coefficient. For simplicity, it is now assumed that each subarea dS_k will be hit by one ray k and contribute with one certain amount of energy c_k at the receiver. Figure 3 gives an illustration of this tessellation.

Further, the arrival time n_k of each ray k will depend on the sum of the distance between the source S and the barrier hit P_k and the distance between the barrier hit P_k and the receiver R. As all rays have reached the receiver an impulse response has been build up by adding all energy contributions, and this impulse response will indeed correspond to (1).

For each ray k, the dedicated energy c_k in (1) will be given by the following formula:

$$c_k = \frac{1}{SP_k \cdot RP_k} \cdot \tau_k \cdot s_k \cdot dS_k \tag{2}$$

where τ_k is the transmission coefficient of the subarea dS_k that ray k propagates through, and s_k is the scattering coefficient out from the noise barrier. These parameters τ_k and s_k will be further discussed in subchapter 3.2. SP_k is the length of the propagation path between the source and the current subarea dS_k, and RP_k is the length of the propagation path between the current subarea dS_k and the receiver.

The value n_k in (1) will be given by the following formula:

$$n_k = \frac{f_s}{c_{air}}\left(SP_k + RP_k\right) \tag{3}$$

where f_s is the sample frequency, and c_{air} is the speed of sound.

Now, given that the number of subareas is large enough, it should in theory be possible to create any desired shape of the impulse response. As the noise barrier is divided into an increased number of subareas, the travel length between two succeeding incoming rays will naturally decrease. Therefore, as the number of subareas grows towards infinity, every relevant sample n of the impulse response $h(n)$ will be the host for a number of energy contributions c_k. Accordingly, the impulse response shape can be calibrated by assigning optimal transmission coefficients τ_k.

In order to assign the parameter τ_k optimal values, it will be a vital task to map all rays/subareas that contribute within the same sample. These will be bounded by a certain barrier projection, centred by the barrier intersection of the direct sound propagation path SR. Figure 3 illustrates the occurring nth sample's barrier relationship.

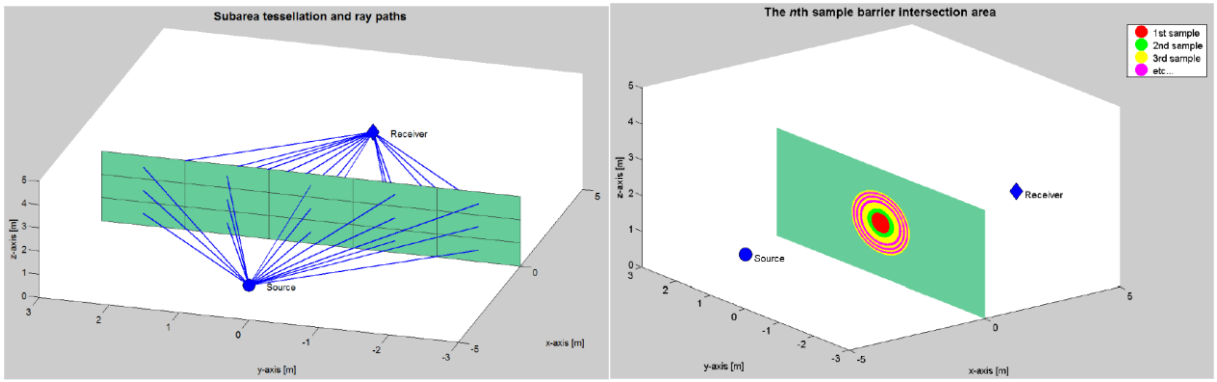

Figure 3: Ray paths of the proposed modelling, and the nth sample barrier intersection area

In theory, the exact shape and size of each *n*th sample barrier intersection area will be bounded by an elliptic radiation pattern quite similar to a Fresnel zone, which in this particular case will be given by the source position $\{S_x, S_y, S_z\}$ and the receiver position $\{R_x, R_y, R_z\}$, as well as the sample frequency f_s and the speed of sound c_{air}. A cross-section of this elliptic zone can be seen in Figure 4.

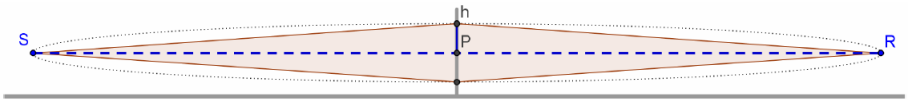

Figure 4: Cross-section of the *n*th sample barrier intersection area

For simplicity, it is now assumed that the *n*th sample barrier intersection area is a circular desk. The *n*th sample barrier intersection area can be found by the following expression:

$$S_n = \pi\left(Ph_n\right)^2 - \sum_{i=1}^{n-1} S_i \tag{4}$$

where Ph_n is the *n*th sample barrier intersection radius that can be expressed by the following formula:

$$Ph_n = \sqrt{2 \cdot \frac{SP \cdot RP}{SP} \cdot \frac{c_{air}}{f_s} \cdot n} \tag{5}$$

3.2 Transmission- and scattering coefficients

Further, a major challenge of the present research will be to dedicate optimal transmission coefficients τ_k to each subarea dS_k. Let's assume for now that the impulse response *h(n)* is known. The global transmission factor of the *n*th barrier intersection area will then be given by the following formula:

$$T_n = \frac{SP \cdot RP}{S_n} \cdot h(n) \tag{6}$$

Consequently, if all subareas that contribute within the sample *n* is dedicated this global transmission coefficient T_n an ideally correct impulse response will be obtained:

$$dS_k \in S \quad \Rightarrow \quad \tau_k = T_n \tag{7}$$

Further, one highly desirable feature in GA is that it should function for any random receiver position simultaneously. Indeed, this should therefore also be taken into account when regarding the semi-transparent design of the noise barrier. One way to implement this feature is by introducing an angle-dependent energy transmission through the wall. For simplicity, it seems favourable to assume a simple cosinus-related scattering pattern:

$$s_k = \cos\varphi_k \tag{8}$$

where φ_k is the ray *k*'s angle out from the subarea dS_k.

Unfortunately, new challenges arise in the search for a semi-transparent modelling that includes this global receiver feature. At present time, the optimal semi-transparent design algorithm remains unknown. Still, one proposed modelling method is presented in subchapter 3.3.

3.3 Proposed method for semi-transparent modelling

The following proposed design algorithm is now employed:

1. A single source and an array of receivers are employed to dedicate transmissions coefficients. In addition to being the source and receivers, these objects, S_G and R_G, will also function as a building kit for the semi-transparent properties of the noise barrier.

2. The noise barrier is divided into two different transmission zones. As known from the quasi-anechoic recording techniques [7, 8, 9], a Fourier transform of the initial samples of a time-smeared impulse response will still give a complete energy representation at high frequencies. Evidently, this can be associated with the ray contributions that arrive earliest at the receiver. Consequently, it can also be claimed that all ray contributions that arrives somewhat further out in the impulse response will only perform an accomplishment of "boosting" the lower frequency energy to a more and more correct energy level. Based on this, the utilized idea is that the *mid/high peak zone* – represented by the earliest incoming rays, raises a somewhat flat frequency response, while the *bass tail zone* – represented by the more time-delayed rays, helps to build the more typical shape of a low pass filter. To illustrate the proposed modelling technique, Figure 5 gives a sketch of the zone division, and the concept of an impulse response being shaped by the two zones. Of course, in practice there will be a more blurred overlap in the transition between the two zone's impulse response contributions, and the final curve shape will be expected somewhat less smooth.

3. The mid/high peak zone: is bounded by the union of the 1st barrier intersection areas of all receivers in the array R_G. Slightly simplified, all the subareas of the mid/high peak zone will now be dedicated a constant transmission coefficients τ_k based on the expected mean peak value of the later achieved impulse responses at R_G. Such peak value knowledge can e.g. be obtained by employing a library, although it would of course be beneficial to develop a more sophisticated mathematical relationship for finding these impulse response peak values (typically based on the simple geometric parameters of Figure 1). However, for simplicity, through the rest of this paper the peak values will be obtained by employing a Matlab toolbox *EDBtoolbox* [10] (developed by the Acoustics Group, NTNU).

4. The bass tail zone: involves all subareas of the noise barrier that are not occupied by the mid/high zone. For simplicity, the bass tail zone is dedicated a constant transmission coefficient that equals to the transmission coefficient of the mid/high peak zone multiplied by a factor *0.1*. The intention is that the continuous damped tail of the impulse response should appear due to the steadily increased spherical propagation damping of succeeding rays, combined with an increased scattering influence.

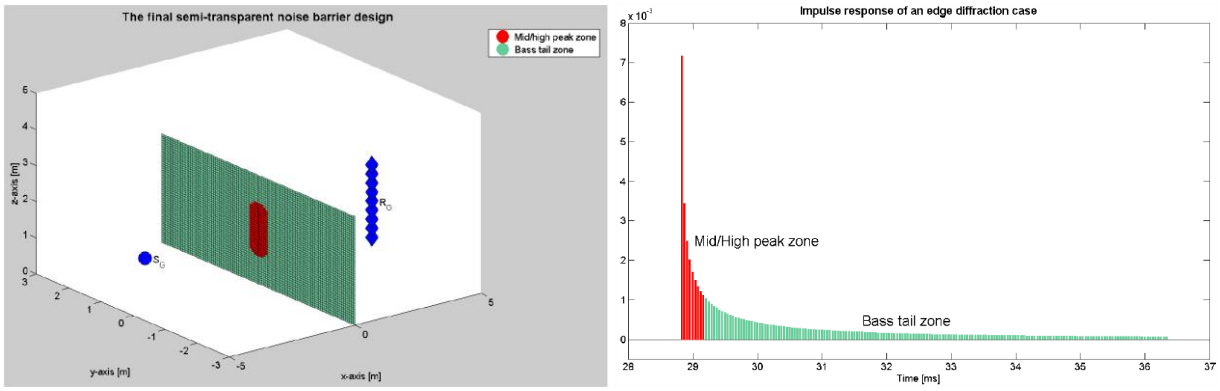

Figure 5: The proposed semi-transparent modelling technique

4 Result

Figure 6 gives a plot of the mean octave band error at the receiver array R_G when S_G is the employed source. The source- and receiver positions were bounded within the intervals $x = [1.0, 30.0]$ *m* and $z = [0.25, 0.75]$ *m*, with a symmetric property regarding the y-axis. In order to present reliable results for general source- and receiver positions, the presented octave band error plots are based on the averaged outcome of a number of 100 simulations series where source- and receiver positions where chosen randomly. As the reference model the already mentioned *EDBtoolbox* [10] was employed.

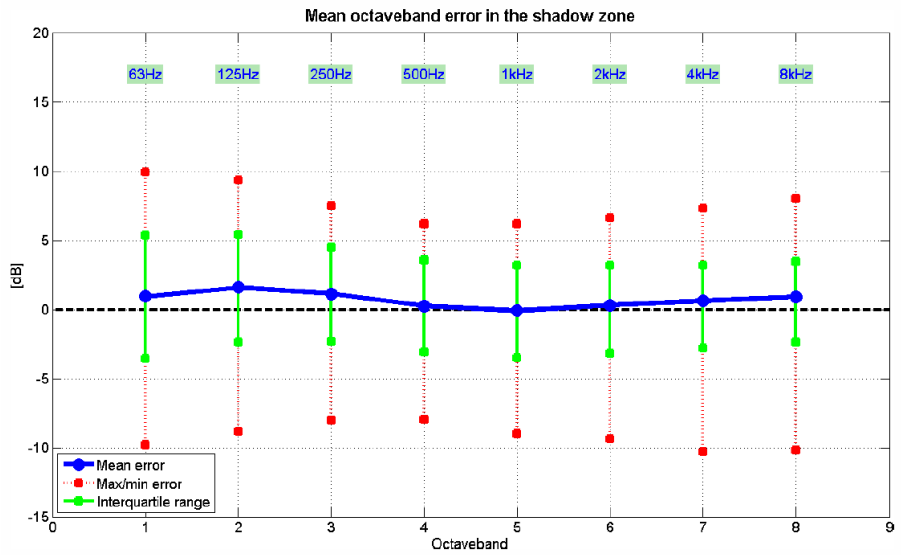

Figure 6: Mean octave band error at the receiver array R_G

5 Discussion

By first impression, it must be argued that the error plot in Figure 6 reveals a fairly hopeful result. The mean errors are very small and almost neglectable. Sadly, large errors are introduced for the max/min-values, as *10 dB* errors cannot be tolerated. The main reason for these errors is probably caused by a general uncertainty in the applied modelling technique. On the other hand, the performed simulation session with randomized source- and receiver positions will certainly include a large amount of critical positions, where it is obvious that the modelling technique will have a limited functionality. Errors are expected for positions very close to the barrier, as well as for positions close to the floor and barrier height. These expected errors are e.g. caused partly due to some assumptions introduced for the *n*th sample barrier intersection area S_n, and partly due to a potentially unfavourable scattering behaviour. Especially, a combination of an odd source and an odd receiver position must be expected to result in a misleading impulse response shape. Fortunately, these unfavourable source- and receiver combinations tend to be rare in any practically relevant case.

Nevertheless, it must also be restated that geometrical acoustics in any case often introduces some errors in the lower octave bands, as room modes, comb filtering effects, etc. are neglected. It could therefore be questioned whether the diffraction errors of Figure 6 at all should be questioned ahead of these already existing uncertainties. Moreover, it will perhaps also be advantageous to implement a mimetic edge diffraction modelling that introduces some uncertainties versus a modelling that yields no edge diffraction energy contributions at all.

However, it must further be assumed that the proposed modelling technique may introduce additional errors that are not revealed by the plot in Figure 6. E.g., one obvious concern arises as the applied symmetric y-axis condition is erased. The mid/high peak zone will then be more smeared out and arrive further out in the impulse response. In addition, the energy contributions c_k of the mid/high peak zone rays will be further affected by the scattering coefficient s_k, due to an increased angle out from the noise barrier. However, this scattering damping may actually not be such a bad approach to how the higher frequencies decrease along the non-symmetric line. Hence, the major concern should most likely be given to the delayed arrival time of the mid/high peak zone rays.

Interestingly, the presented modelling is based on a broadband simulation technique, which to some extent is advantageous, but which also will cause some issues regarding a potential GA software implementation. Normally, to imitate a frequency-dependent absorption property of surfaces, simulations are run separately for each octave band. From there, the echogram values of each octave band are post-processed to form an interpolated frequency response. Finally, this frequency response is combined with a DSP filter to generate a continuous broadband impulse response curve. Accordingly, the question is how a broadband simulation technique can be implemented in this applied octave band simulation technique? One possible solution could perhaps be to run a separate "edge diffraction" simulation in addition to all the octave band simulations, and then somehow merge the edge diffraction impulse response to the final output impulse response by post-processing. By contrast, one obvious alternative modelling technique could be to develop a noise barrier design that involves an octave band-based transmission coefficient. Such a solution corresponds to both the previous semi-transparent edge diffraction modelling studies by *Dammerud* [2] and *Isebakke* [3].

Further studies should also be performed regarding the reverbant consequences of the presented edge diffraction modelling. In this study only early edge diffraction energy contributions are considered. How is the often present reverberation field affected by this modelling technique? Moreover, since this is a broadband simulation method, what will happen as these rays hit a frequency-dependent absorptive surface?

6 Summary

To summarize, a general potential in the proposed semi-transparent edge diffraction modelling technique has been revealed. The presented results and discussion indicate a somewhat successful modelling of the infinite noise barrier edge diffraction case. However, some unwanted errors are introduced at rare source-receiver positions. Thus, possible future studies should be performed in search for a somewhat improved modelling algorithm.

So far, no attempt has been made to implement the proposed edge diffraction modelling in commercially available GA software. Some possible complications are introduced as the presented modelling is a broadband ray-tracing simulation method, whereas the common procedure is to perform individual octave band simulations. In conclusion, further research should study to which extent the proposed modelling technique actually can be implemented in commercial GA software.

A main outcome of this report reveals that a fairly satisfying model of the noise barrier edge diffraction case can be developed based on knowledge about the expected impulse response peak values. Accordingly, there should be of further interest to find a somewhat simple relationship between the impulse response peak value and the simple geometry of the given infinite noise barrier case.

References

[1] U. P. Svensson, R. I. Fred & J. Vanderkooy, *An analytic secondary source model of edge diffraction impulse responses*, J. Acoust. Soc. Am. 106, 2331-2344, 1999.

[2] J. J. Dammerud, *Stage acoustics for symphony orchestras in concert halls*, Ph.D. thesis, University of Bath, England, 2009.

[3] A. Isebakke, *Modelling audience seating area in geometrical room acoustic software*, Faculty of information technology, mathematics and electrical engineering, Norwegian university of science and technology, Norway, 2010.

[4] A. Krokstad, S. Strøm & S. Sørsdal, *Calculating the acoustical room response by the use of ray tracing technique*, J. Sound and Vibration 8, 118-125, 1968.

[5] CATT-Acoustic, *CATT-Acoustic v8.0 user's manual*, 2002.

[6] CATT-Acoustic, *Addendum to CATT-Acoustic manual*, 2010.

[7] J. M. Berman & L. R. Fincham, *The application of digital techniques to measurement of loudspeakers*, J. Audio Eng. Soc. 25, 370-384, 1977.

[8] L. R. Fincham, *Refinements in the impulse testing of loudspeakers*, J. Audio Eng. Soc. 33, 133-140, 1985.

[9] E. Benjamin, *Extending quasi-anechoic electroacoustic measurements to low frequencies*, AES Convention paper 6218, 2004.

[10] U. P. Svensson, "*http://www.iet.ntnu.no/~svensson/software/index.html*"